*Arctic, Antarctic, and Alpine Research, Vol. 40, No. 2, 2008, pp. 323–334*

# General Characteristics of Temperature and Humidity Variability on Kilimanjaro, Tanzania

*W. J. Duane**
*N. C. Pepin†*
*M. L. Losleben‡ and*
*D. R. Hardy§*

*Department of Geography, Universiti Brunei Darussalam, Jalan Tungku Link, Gadong, BE1410, Brunei Darussalam
†Corresponding author: Department of Geography, University of Portsmouth, Lion Terrace, Portsmouth, Hants PO1 3HE, U.K.
nicholas.pepin@port.ac.uk
‡National Phenology Network, National Coordinating Office, 1955 East Sixth Street, Tucson, Arizona 85719, U.S.A.
§Climate System Research Center, Department of Geosciences, University of Massachusetts, Amherst, Massachusetts 01003, U.S.A.

## Abstract

Hourly temperature and humidity observations were obtained over 16 months from loggers ranging in elevation from 1890 to 5800 m a.s.l. up the southwestern slope of Kilimanjaro, Tanzania. The vertical gradient in mean air temperature is non-linear, with the treeline weakening the gradient and the snow-ice line enhancing it. On average, moisture availability (both relative humidity and absolute vapor pressure) decreases with elevation, but the seasonal and diurnal variability in relative humidity (RH) is enhanced toward the mountain summit. The strong diurnal cycle in humidity is shown to be an outcome of strong upslope moisture transport during the day, counterbalanced by downslope transport and drying at night. Cooling on the lower slopes during the months of June and July weakens the lapse rates and consequently convective activity. This is borne out by the reduction in cloud amounts (using a surrogate threshold of RH $> 95\%$), toward the summit during these months. The lower slopes of Kilimanjaro are observed to be a major moisture source for the summit region, and implications of this for the mass balance of the summit glaciers are discussed.

DOI: 10.1657/1523-0430(06-127)[DUANE]2.0.CO;2

## Introduction

The impact of any climate change on high altitude regions is of fundamental importance to the region itself, its resources, and its surrounding environments (e.g. Hastenrath, 2001; Bradley et al., 2006). There is evidence in some environments that global warming may be amplified at high elevations (Bradley et al., 2004; Diaz and Bradley, 1997), although this may not be universally applicable (Pepin and Seidel, 2005). While much work has been concerned with northern hemisphere mountain regions, e.g. Rocky Mountains and the European Alps, little examination has been undertaken of the less populated mountain regions, especially in the tropics. This work introduces the analysis of temperature and humidity regimes on an isolated mountain, Kilimanjaro (3.07°S, 37.35°E, 5892 m), lying approximately 340 km south of the equator. Considered to be the highest free-standing mountain in the world, it gives an ideal location to examine the vertical variability of these two climatic factors and their relationship to theoretical models of mountain thermal circulation (Troll and Wien, 1949). Associated with this is the widespread concern about the retreat of the summit glaciers (Kaser et al., 2004; Cullen et al., 2006). A more thorough investigation of present temperature and humidity regimes on the mountain will help this enquiry.

This paper demonstrates the characteristics of the present temperature and humidity patterns at the local scale. After the regional setting is outlined, and methods of data collection discussed, the analyses are divided into five main sections, outlining (a) the steps taken to give confidence to the collected data, (b) general elevational contrasts in both temperature and humidity, (c) seasonal contrasts, (d) a more detailed discussion of temporal (particularly diurnal) variability, and (e) a discussion of cloud and moisture regimes. A central theme is the association between cloud and moisture variability at various heights up the mountain and its relationship with air temperatures. The relevance of our research to the debate concerning glacier behavior is then presented.

## Regional Climate

The main factor influencing the climate of East Africa is its proximity to the equator and hence the influence of the trade wind regime, controlled by movement of the intertropical convergence zone (ITCZ). The ITCZ follows the band of most positive net radiation around the globe that produces the greatest convection (Hills, 1979). During the austral summer the ITCZ lies to the south of the equator, introducing northeasterly trade winds into Kenya and Tanzania, while the boreal summer, with the ITCZ lying to the north, produces southeasterly trade winds. The transition between these trade wind regimes produces two periods of enhanced rainfall, the 'long rains' during March to May, and the 'short rains' in October and November. These periods occur when the ITCZ is located approximately over the equator, also contemporaneous with times of average monthly temperature maxima. Inter-annual variability of the 'short rains' and their associated moisture is associated with the ENSO signature (Ropelewski and Halpert, 1987), which modulates sea surface temperature anomalies in the Indian Ocean (Latif et al., 1999). Kabanda and Jury (1999) used meridional and zonal wind flows in the Indian Ocean plus the southern oscillation index in a regression model to account for over half of the interannual variability in the rainfall during the 'short rains.' Mölg et al. (2006) linked the interannual variability of the 'short rains' with Indian Ocean Zonal Mode activity identified by anomalous warming (cooling) in the western (eastern) Indian Ocean, which produces enhanced convection in East Africa. The East African Low Level


1523-0430/08 $7.00

**FIGURE 1. Logger 9 (5470 m a.s.l.), showing the horizontal positioning of the radiation shield, oriented north-south to prevent shortwave radiation influx. The shield's diameter:length ratio was chosen to permit adequate shading yet sufficient ventilation of the sensor.**

Jet (EALLJ), centered at an altitude of approximately 1.5 km, may influence the climate of Kilimanjaro, particularly around the months of June and July when the jet is at its maximum both in terms of velocity and penetration inland from the Indian Ocean (Findlater, 1977).

Kilimanjaro has a tropical equatorial climate modified by altitude, thus its vertical extent allows for a range of climatic zones to exist within a relatively short distance. Although this altitudinal zonation is dominant, there is also some distinction based upon aspect, with enhanced rainfall on the southern side of the mountain. Hemp (2002) used the vertical distribution of pteridophytes along 24 transects on the southern slopes to define climate zones. The major zones include a submontane zone below 1600 m, a montane zone (1600–2800 m), a subalpine zone (2800–3900 m), and an alpine zone (above 3900 m). Rainfall distribution, derived from empirical data by Rohr and Killingtveit (2003), shows a maximum at about 2200 m a.s.l. Further work by Hemp (2005a) agrees with the elevation of maximum precipitation, although the vertical distribution of precipitation amounts differs.

## Data and Methods

Ten Onset Hobo Pro Data Loggers were deployed, measuring temperature and relative humidity (RH) with quoted accuracies of $\pm 0.2^{\circ}$C at 20°C, and $\pm 3\%$ in a non-condensing environment ($\pm 4\%$ in a condensing environment). Prior to deployment all loggers were compared across a range of temperatures and relative humidities with differences between loggers being negligible ($<0.15^{\circ}$C and $<1\%$ RH) in comparison to the environmental differences being measured on the mountain. Partial pressures of water vapor (vapor pressures) were calculated from air temperatures and relative humidities using equations in Kuemmel (1997). Loggers were positioned 1.5 m above ground level within a 25-cm-long, 2-mm-thick cylindrical uPVC radiation shield positioned horizontally with open ends oriented north and south to shelter the instrument from direct sunlight (see Fig. 1). The sampling interval was set at 1 hour, giving over 11,600 observations for the data period between September 2004 and January 2006.

The locations of the 10 sites are shown in Figure 2 and details given in Table 1. They follow a profile up the southwestern side of the mountain within the limits of Kilimanjaro National Park, with all locations having similar aspect and avoiding topographic hollows. Loggers 1 and 7 were lost and logger 6 did not operate, leaving 7 loggers to provide data over an elevation range of 3910 m. The missing and malfunctioning loggers have since been replaced to contribute to the existing network, thus increasing the spatial and temporal coverage. To aid in understanding the environment, Figure 3 shows four major altitudinal zones illustrating the distribution and abundance of vegetation with elevation.

## Analyses

### *DATA VALIDATION*

While a detailed comparison of our Hobo logger data with free-air data, both radiosonde and reanalyses, is beyond the scope of this paper, a quick comparison with daily radiosonde ascents from Nairobi (220 km north of Kilimanjaro) is shown in Figure 4. Ascents were obtained from the Integrated Global Radiosonde Archive (IGRA) published by the National Climate Data Center (NCDC, 2007) for 293 days during our monitoring period, including all seasons of the year. Details and development of the IGRA data set have been discussed by Durre et al. (2006). Because the available ascent is at 23:00 UTC (02:00 East African Time [EAT]), the mountain is colder than the free atmosphere. This is in accordance with Dreiseitl (1988), who found similar nocturnal differences (in the order of 2°C) at elevations above 1500 m in the Alps, and agrees with other studies (Pepin and Losleben, 2002; Pepin and Seidel, 2005). However, differences become greater (3–5°C) at lower altitudes within the rain forest. A rapid transition between loggers 4 and 5 (3170 and 3630 m, respectively) is suggestive of a change from the nocturnal boundary layer to a more free-air-dominated regime (for a detailed review of global free air/surface temperature contrasts and their relationship to elevation and topography, see Pepin and Seidel, 2005). Site 10 does not fit the general trend, showing greater nocturnal cooling over the icefield caused by the heat sink effect of the ice (Mölg and Hardy, 2004). The standard deviation of the temperature difference also decreases with elevation as the strength of free-air advection increases.

Logger 10 was situated on the same mast as a Rotronics MP101A temperature and humidity sensor housed in an aspirated radiation shield on the Northern Icefield. Hour-on-hour comparisons were made between the raw data over the full observation period, yielding *r*-values (Pearson product-moment correlation coefficients) of 0.88 for temperature and 0.94 for relative humidity. Some of the difference may be attributable to the difference in sampling strategies. The Hobo logger takes instant readings at each hour while the Rotronics sensor takes the mean values over the hour. Unknown timing differences (e.g., clock errors on Hobo

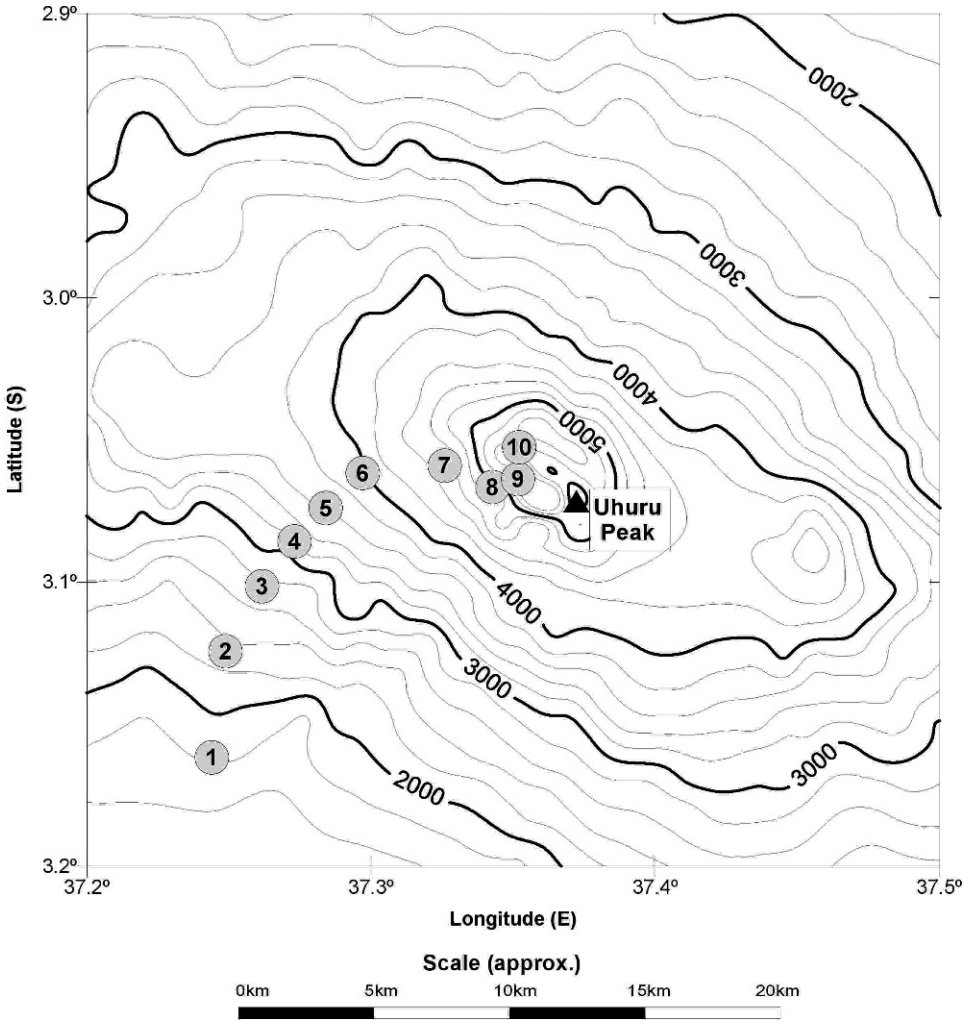


**FIGURE 2. Map showing location of the 10 logger sites on the south-western slopes of Kilimanjaro.**

loggers can only be determined to the precision of the sampling interval, in this case one hour) may also be partly responsible for differences between measurements, particularly at sunrise and sunset when temperatures change more rapidly. Solar radiation at the logger 10 site is extreme, typically reaching 1100 W $m^{-2}$ at midday. The Hobo sensor is influenced by solar heating more than the Rotronic sensor but the difference is small. The mean (inter-instrument) difference in daily maximum temperatures (when this effect would be most noticeable) is 0.9°C and at least part of this difference would be a result of the lower instrument height of the Hobo. The absolute heights above the ice surface vary with the change in snow/ice levels, but the Hobo logger is situated ~1 m below the Rotronic sensor. Daily mean temperatures were in good agreement ($r = 0.95$). This analysis and the comparison with radiosonde data provide confidence that our Hobo instruments are faithfully recording environmental air temperature and humidity. Radiative errors would be smaller at lower sites, and further confidence is provided by having identical systems at all of our stations.

### *ALTITUDINAL VARIABILITY*

Table 2 shows overall changes in temperature and relative humidity with elevation. Lapse rates are expressed as negative when temperatures decrease with elevation (the normal situation). The average lapse rate is −5.1°C $km^{-1}$ but there is some variability. Traveling up through the rain forest, the lapse rate becomes shallower, reaching a value of −1.4°C $km^{-1}$ around 3500 m in the vicinity of the treeline. Across the subalpine and alpine zones the lapse rate steepens slightly, but it is at the crater rim where it abruptly steepens to −10.3°C $km^{-1}$. Different processes are responsible for these changes at different elevations. Mean temperatures in the rain forest are reduced by cooling processes through absorption and reflection of solar radiation in the canopy, extensive and persistent cloud cover, precipitation, and high evapotranspiration. Hemp (2005a) indicates a rainfall maximum of 2700 mm at 2200 m, falling to 1000 mm at approximately 3200 m. These surface cooling processes weaken toward the subalpine zone, giving a sudden decrease in the lapse rate at the treeline.

Site 4 shows an enhanced diurnal temperature range, in particular becoming warmer than sites 2 and 3 during the daytime, but substantially cooler at night. A daytime inversion between sites 3 and 4 is likely a result of the decrease in vegetation cover between these two locations, site 4 having fuller exposure to direct radiative exchanges due to an increased sky-view factor as evidenced by Figures 3a and 3b. Site 4 is also cooler than site 5 at night, and the lack of any bowl-like topography suggests that cold-air ponding is unlikely to be a cause. The difference may be representative of a transition between a cooler, stiller boundary layer–dominated regime at lower elevations and a warmer free air regime controlled by mixing at higher elevations (also suggested by Fig. 4), but the detailed mechanisms require further research. The enhanced temperature difference between sites 9 and 10 primarily reflects site differences, as detailed in the next paragraph.

**TABLE 1**

**Details of logger sites.**

| Logger No. | Elevation (m) | Site description |
|---|---|---|
| 1 | 1890 m | Dense montane rainforest |
| 2 | 2340 m | Dense montane rainforest |
| 3 | 2760 m | Sparse montane rainforest |
| 4 | 3170 m | Transitional zone between rainforest and subalpine heathland |
| 5 | 3630 m | Subalpine heathland |
| 6 | 4050 m | Alpine with limited vegetation |
| 7 | 4570 m | Alpine with limited vegetation |
| 8 | 4970 m | Bare rock |
| 9 | 5470 m | Bare rock |
| 10 | 5800 m | Ice field |

A detailed breakdown of the mean temperature, relative humidity, and vapor pressure profiles is also shown in Figure 5. For mean temperatures (Fig. 5a) there is a general decrease with increasing elevation with the exception of the area between 3000 and 3500 m where there is no appreciable change. This is also a region of increased temperature variability as shown by the divergence between 5th and 95th percentiles and the standard deviation curve. This region coincides with the ecotone between the rain forest and heathland. The lapse rate of mean temperature shows variability with shallower regions around 3400 and 5200 m and a steeper region toward the maximum elevation at 5800 m. The first shallow region is related to the increased ecotone-induced variability mentioned above, while the second shallow region may be a result of topographical forcing and/or surface type. There is a rapid change in temperatures between the sheltered debris field at site 9 and the icefield at site 10 due to variable exposure to airflow patterns (sudden increased exposure to the free atmosphere at site 10) and differences in surface conditions (see Table 1 and Fig. 3).

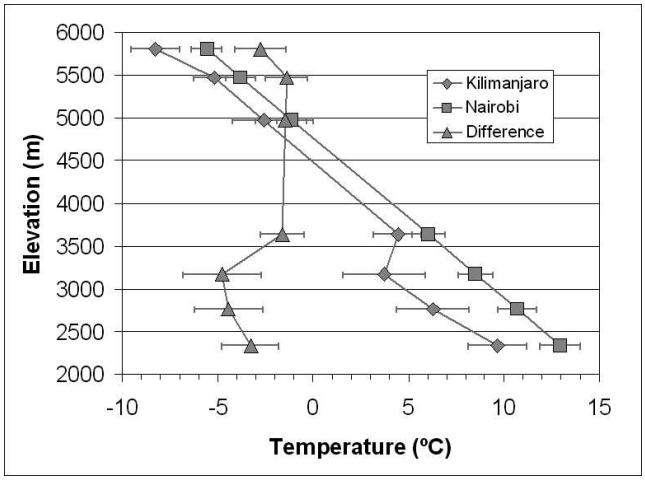


**FIGURE 4. Comparison of average 02:00 EAT logger temperatures with radiosonde data launched at the same time at Nairobi, with ±1 standard deviation bars.**

Relative humidities are shown in Figure 5b. On rare occasions figures slightly over 100% are recorded when the sensor becomes wet. The study period incorporates three wet seasons

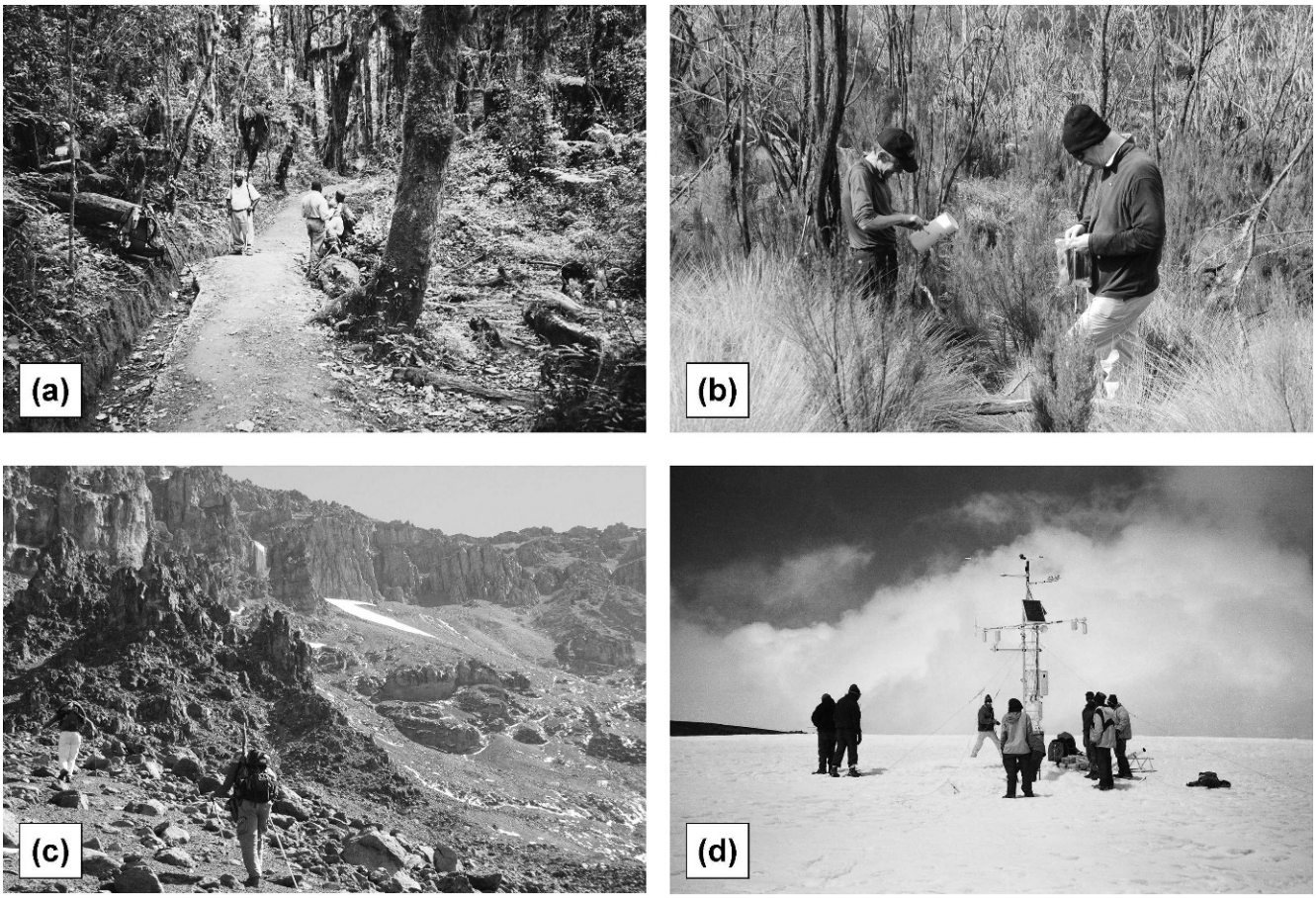


**FIGURE 3. Photographs showing exemplar altitudinal zonation on Kilimanjaro. (a) Montane forest, (b) subalpine heathland, (c) alpine, and (d) icefield. These correspond to the upper three zones of Hemp (2002) and the nival zone.**

**TABLE 2**

**Overall mean temperatures, mean daily minimum and maximum temperatures and mean relative humidity at each location. Lapse rates (°C km$^{-1}$) are derived based on comparison with the immediate station below.**

| | Air Temperature (°C) | | | | | | Relative Humidity (%) |
|---|---|---|---|---|---|---|---|
| Logger No. | Mean | Lapse Rate | Min | Lapse Rate | Max | Lapse Rate | Mean |
| 2 | 11.5 | | 8.4 | | 14.8 | | 97.7 |
| 3 | 9.2 | −5.6 | 4.9 | −8.3 | 14.4 | −0.9 | 96.0 |
| 4 | 7.8 | −3.5 | 1.9 | −7.3 | 15.5 | 2.7 | 88.9 |
| 5 | 7.1 | −1.4 | 3.3 | 3.0 | 13.3 | −4.8 | 77.3 |
| 8 | −0.9 | −6.0 | −3.9 | −5.4 | 3.4 | −7.4 | 65.5 |
| 9 | −2.8 | −3.8 | −6.0 | −4.2 | 2.4 | −2.0 | 56.0 |
| 10 | −6.2 | −10.3 | −9.4 | −10.3 | −2.0 | −13.3 | 54.4 |

(OND 2004, MAM 2005, and OND 2005) but only one lengthy dry period (JJAS 2005), which may result in higher relative humidity values than climatological means. Mean relative humidities show a general decrease with elevation but also an increase in variability toward the summit. This could be taken to suggest that moisture availability is sporadic in the higher reaches of the mountain. However, much of this variability does not represent the amount of moisture since vertical profiles of absolute vapor pressure (Fig. 5c) do not show the same increase in variability. Lower temperatures in the summit region mean that equivalent changes in absolute vapor pressure have a larger effect on relative humidity. Thus cloud development/dispersal can be triggered by a small import/export of moisture which enhances the consequences of atmospheric moisture variability near the mountain summit. The standard deviation of vapor pressure is reduced at the highest site, possibly due to sublimation from the snow and ice (Mölg and Hardy, 2004).

Given stable conditions with limited advection, we would expect the correlation between air temperature and relative humidity at any one location to be negative, and if vapor pressure were constant this relationship would be determined. On Kilimanjaro the overall correlations between temperature and relative humidity at each site decrease with elevation. Examination of selected scatterplots (Fig. 6) shows that there are two types of regime. The first is dominated by a strong negative relationship between air temperature and humidity (for example at site 3), implying relatively constant vapor pressure and warming/cooling of air *in situ*. This is prevalent on the lower slopes. The other regime type is where there is no relationship between temperature and relative humidity. This is more common on the higher slopes (example site 10). Sites 5 and 8 show transitional behavior between conditions on upper and lower slopes. This suggests there may be a stable *in situ* regime below a subsidence inversion where there is limited air mixing, and a more vigorous advective regime above the

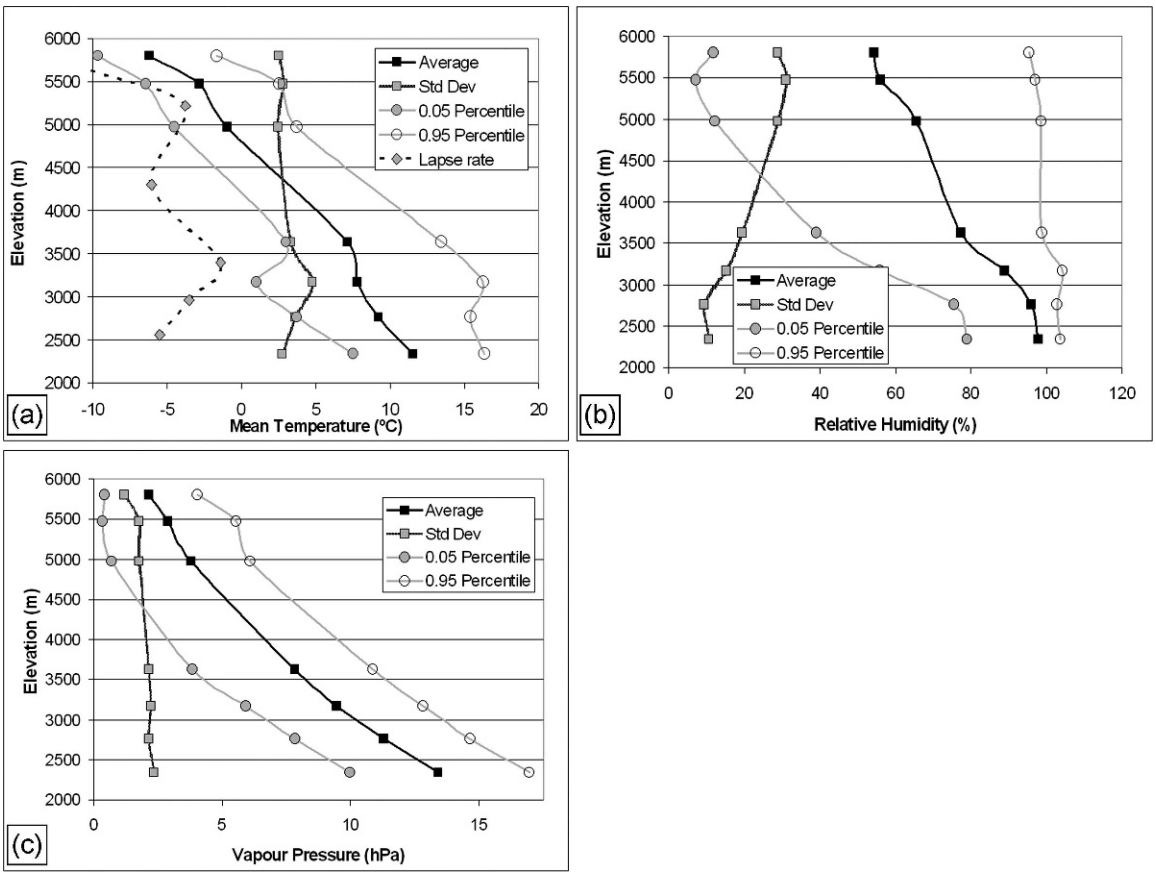


**FIGURE 5. Vertical profiles of (a) mean temperature, (b) relative humidity, and (c) absolute vapor pressure. Percentiles are taken from hourly observations.**

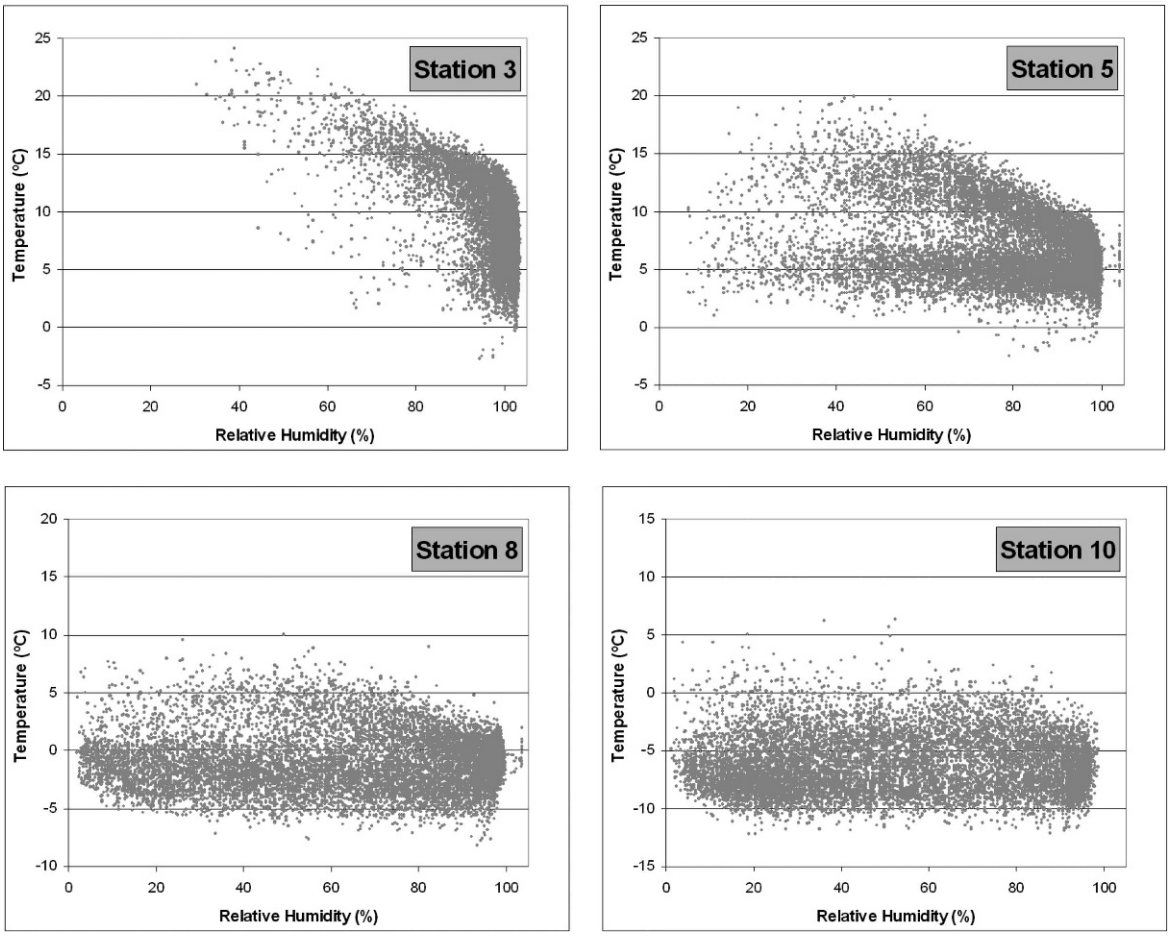


**FIGURE 6. The relationship between air temperature and relative humidity at four selected sites.**

inversion where upslope/downslope flow will import or export atmospheric moisture to/from the higher elevations. Site 5 is again critical, typifying the transition zone which can be part of both regimes.

The spatial homogeneity of temperature variance up the mountain was measured through derivation of the temperature anomaly correlation between adjacent sites. This method allows identification of logger locations with similar temperature regimes (Table 3). Of particular interest is the uniformity of the regime in the rain forest (sites 2, 3, and 4) and the reduction in intersite correlations at the higher levels of the mountain (despite smaller absolute elevation differences). This suggests that synoptic forcing has a spatially heterogeneous influence above treeline (probably through topographically induced cloud cover variation and/or differential exposure to advection), but that at lower levels the tree cover stabilizes temperature responses to radiation fluxes reducing intersite contrasts. The anomaly correlation between the top and bottom sites is extremely low, showing contrasting temperature regimes at the top and bottom of the mountain.

**TABLE 3**

**Hourly anomaly correlations between pairs of logger sites.**

| Logger Pair | Temperature Anomaly Correlation | Elevation Difference (m) |
|---|---|---|
| 2-3 | 0.811 | 420 |
| 3-4 | 0.742 | 410 |
| 4-5 | 0.544 | 460 |
| 5-8 | 0.131 | 1340 |
| 8-9 | 0.432 | 500 |
| 9-10 | 0.317 | 330 |
| 2-10 | 0.051 | 3460 |
| 2-5 | 0.242 | 1290 |
| 8-10 | 0.108 | 830 |

### *SEASONAL VARIABILITY*

Monthly mean temperatures, relative humidities, and vapor pressures for each logger are shown in Figure 7. The temperature plot indicates a stronger seasonal signature at lower altitudes. There is a general cooling trend during June to August coinciding with austral winter and aphelion, as well as the dry period between the long and short rains at the lower sites. This is less evident at elevations above 3000 m, indicating that there may be some impact from the EALLJ. Particularly noticeable is the isothermal behavior between sites 4 and 5 for this period. Further analysis, comparing average monthly daily maximum and minimum temperatures (not shown) shows that the maximum temperature has the larger seasonal contrast, particularly for sites 2 and 3 within the rain forest. The mean diurnal temperature range at Site 2 in July falls to 3.4°C, compared to 9.5°C at the same site in February. This is predominantly due to the fall in daily maxima in July which is related to a persistent layer of stratocumulus cloud which forms underneath a subsidence inversion trapping lower level moisture in the southeast trade winds (Griffiths, 1972; Kuhnel, 1991; Plisnier et al., 2000). The monthly lapse rate, calculated using sites 2 and 10, therefore, shows a seasonal signature steepening around December when conditions are dry and becoming shallower around July. Again, the seasonal lapse rate trend is dominated by the temperature variation at lower altitudes.

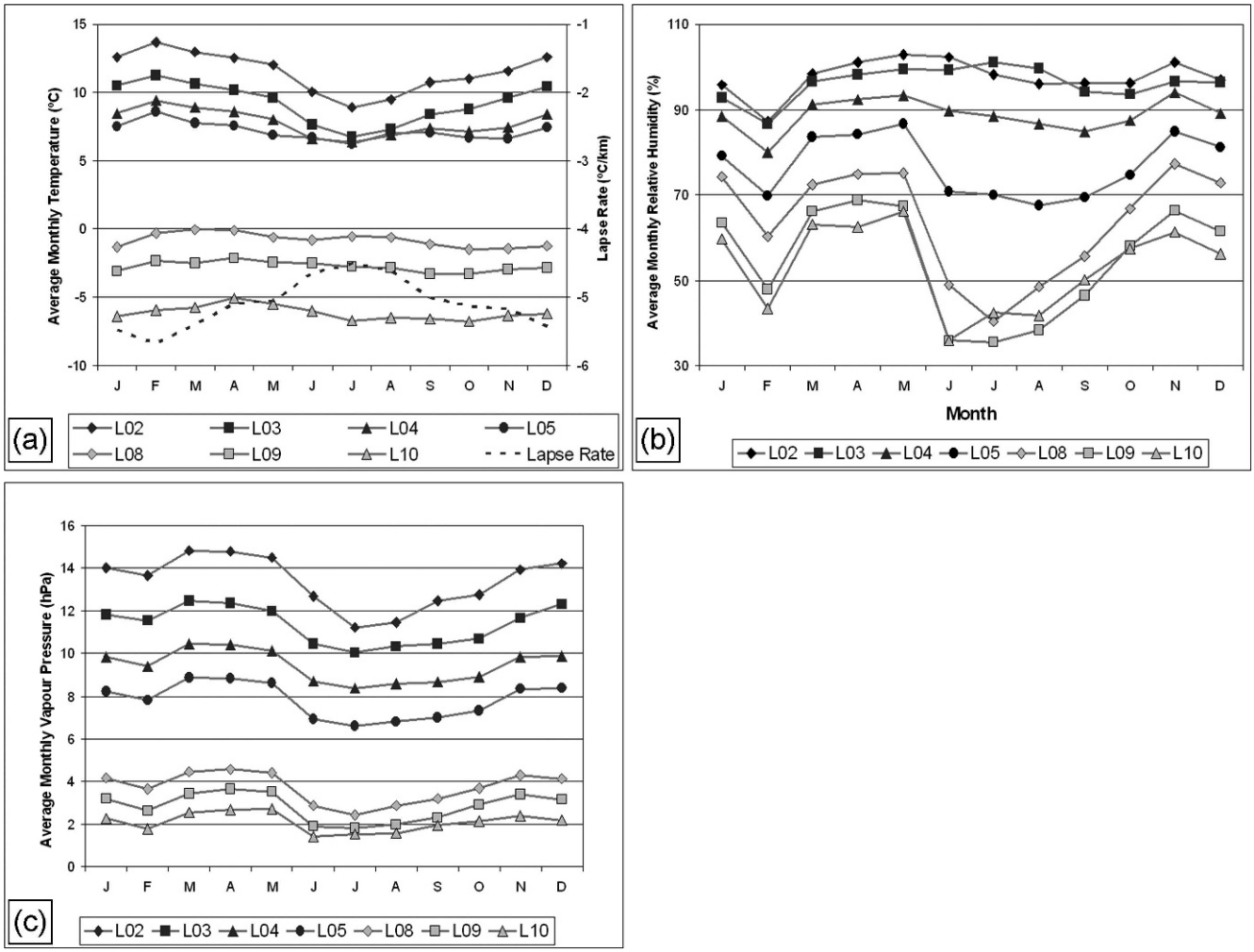


**FIGURE 7. Monthly variation of (a) mean air temperatures, (b) mean relative humidity, and (c) mean absolute vapor pressure.**

Monthly mean relative humidities also show a seasonal signature (Fig. 7b), producing maxima during the rainy seasons at all altitudes, but in contrast to temperature, the strongest seasonality is seen at higher altitudes. This highlights the importance of synoptic forcing in creating the necessary instability to transport moisture to the higher levels of the mountain. The higher altitudes show their least humid period during the June–September dry season, whereas the lower altitudes show their least humid period during the January–February dry season. On the other hand, seasonal vapor pressure variability (Fig. 7c) is considerably dampened with consistent altitudinal gradients throughout the year. The general trend follows the rainfall cycles with the driest period around June to August. This period is particularly noticeable at lower altitudes, again possibly due to the influence of the EALLJ.

This seasonal contrast is also further supported by a comparison of diurnal profiles of temperature, relative humidity, and vapor pressure in January and July (Fig. 8). The temperature difference between the two seasons (January minus July) reverses sign between the top and bottom sites (Fig. 8a). Relative humidity differences (Fig. 8b) are also mostly stratified by elevation. Vapor pressure differences (Fig. 8c), however, peak at site 5 and are universally positive. They are also accentuated during daylight at all locations except site 10. The daytime accentuation suggests that much of the seasonal difference could be the result of variable upslope moisture advection. The heathland zone, where vapor pressure differences are largest, requires further investigation.

Stronger upslope advection could be due to the slightly stronger solar heating in January (compared with July). The variation in sun-Earth distance could contribute to this contrast, even though the difference in noon solar elevation is small (about 6°). The southwesterly aspect would enhance the seasonal contrast in surface radiation receipt on our transect but without data for the other sides of the mountain (where this would not be the case) it is difficult to substantiate the exact cause. It is clear that direct observations of the thermal circulation in the vicinity of at least some of our logger locations, e.g. anabatic and katabatic flows, their changeover, and correlation with moisture fluxes should be a focus for further research efforts.

### *DIURNAL VARIABILITY*

In the tropics the diurnal cycle is often far more pronounced than seasonal contrasts and, as such, characterizes the climate on Kilimanjaro. Figure 9a shows the mean diurnal temperature regime at each site based on mean hourly observations over the whole 16 months. Many of the lower sites show rapid warming in the two to three hours after dawn (approximately 06:30 EAT), with daytime maxima occurring as early as 10:00 EAT at sites 3, 4, and 5. Thereafter it is assumed that cloud development often prevents further warming at these sites. Site 2 within the rain forest (and typically below the cloud base for much of the day) shows a more normal extended daily progression, with a maximum at 16:00 EAT. The upper sites, with the exception of site 10 which shows an idealistic bell-shaped response to short-wave radiation

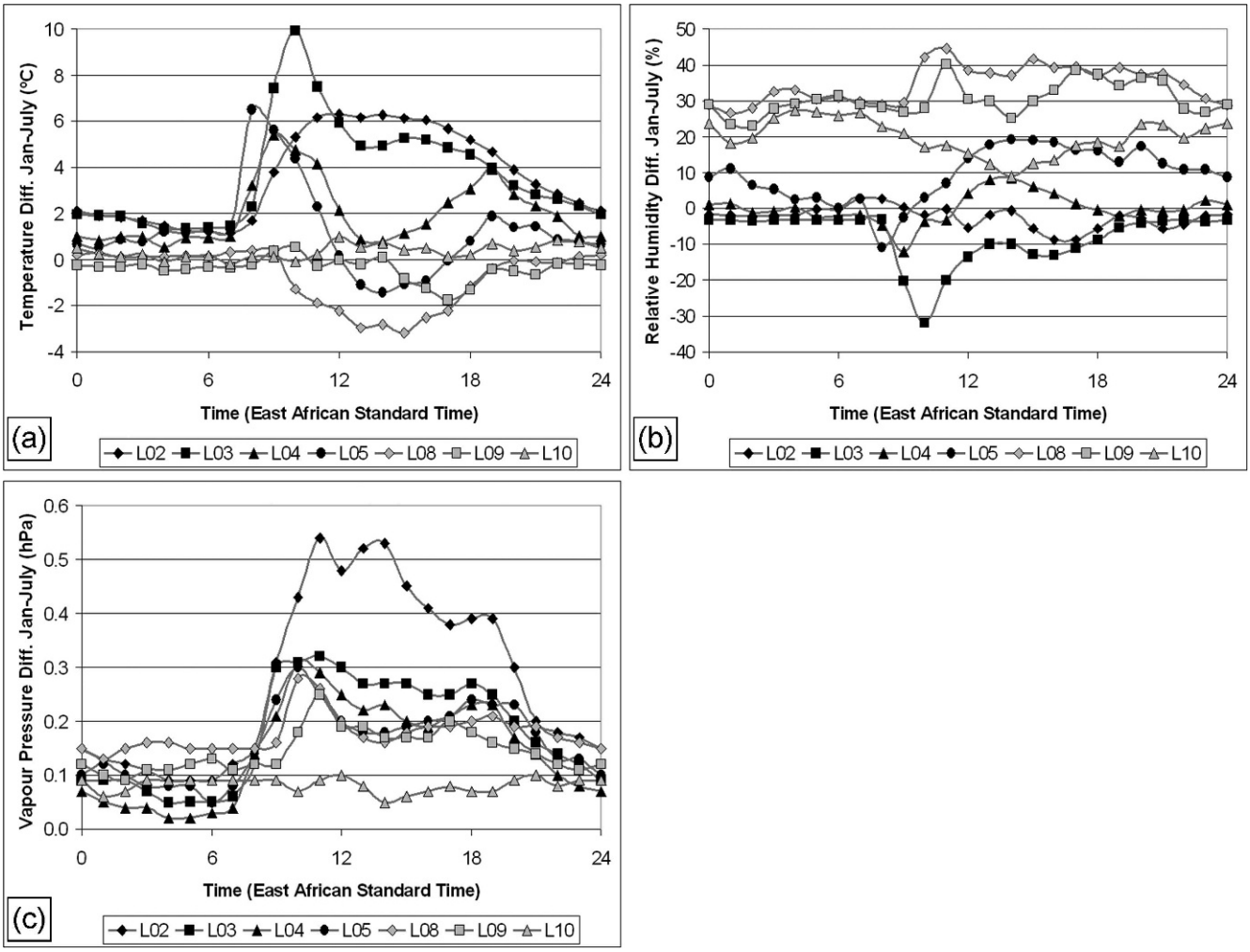


**FIGURE 8. Mean diurnal regime of differences (January minus July) of (a) air temperature, (b) relative humidity, and (c) vapor pressure.**

flux, show limited temperature change during daylight hours, presumably due to a combination of increased free-air advection and/or cloud development. For example, air temperature at site 9 stays more or less constant from 10:00 until 17:00 EAT.

The daily cycles of relative humidity vary considerably according to elevation (Fig. 9b). At site 2 the relative humidity is consistently high, only dropping a little in the afternoon, suggestive of persistent cloud cover with the cloud base rising above this elevation or the stratiform cloud dispersing somewhat during the heat of the day. As we progress upslope a morning decrease in relative humidity develops, suggesting subsidence of the cloud top below the elevation concerned at the end of the night. This signifies evidence of nocturnal downslope katabatic flow, particularly apparent at site 5. The prominent morning minima at sites 3, 4, and 5 are probably caused by the initial increase of solar energy as the sun rises, also evidenced by the rapid increase of temperature in Figure 9a. Subsequent diurnal increases are through evapotranspiration and upslope moisture transport. The low humidities become increasingly more pronounced towards the subalpine zones so that at site 5 the relative humidity remains below 80% for the entire morning. The major feature of upper level sites is the reversal of the daytime minimum in relative humidity (seen at site 2) to a daytime maximum. At sites 8, 9, and 10 daytime is more humid than nighttime in both relative and absolute terms. Taken together this shows the importance of slope convection transporting moisture up the mountain during daylight hours. The patterns in humidity fit in with the conceptual model of tropical mountain circulation of Troll and Wien (1949). In their model (p. 272), the cloud base rises in the afternoon, meaning that sites in the forest zone will show a minimum in relative humidity then (e.g. site 2). At night the cloudy zone both descends in elevation and contracts with downslope flow above the cloud top suppressing its upper limit, thus explaining the minimum in relative humidity at sites 4 and above in the early morning.

Although relative humidities are extremely useful for understanding cloud formation, their dependence on air temperature can confuse the interpretation of atmospheric moisture changes. Mean cycles of vapor pressure (Fig. 9c) show similar daytime peaks at all elevations (with the possible exception of site 10), again showing upward transport of vapor due to slope convection at all levels during the morning, and downward transport due to subsidence later in the day and at night. The transport of moisture from the lower slopes can be seen from Figure 9d where the morning rate of increase in vapor pressure on the upper slopes shows a lag of approximately two to three hours behind the increase on the lower slopes. Likewise, the leveling off in the increase (approaching a constant vapor pressure value) again shows a similar lag of approximately two hours. The downslope movement of moisture appears slightly more complex, although a lag is apparent between sites 9 and 8. The uniqueness of site 10 shows evidence of a distinct modification by the glacier and/or free air circulation. Thus extrapolation of climatic conditions to glacier level from lower elevation sites is risky.

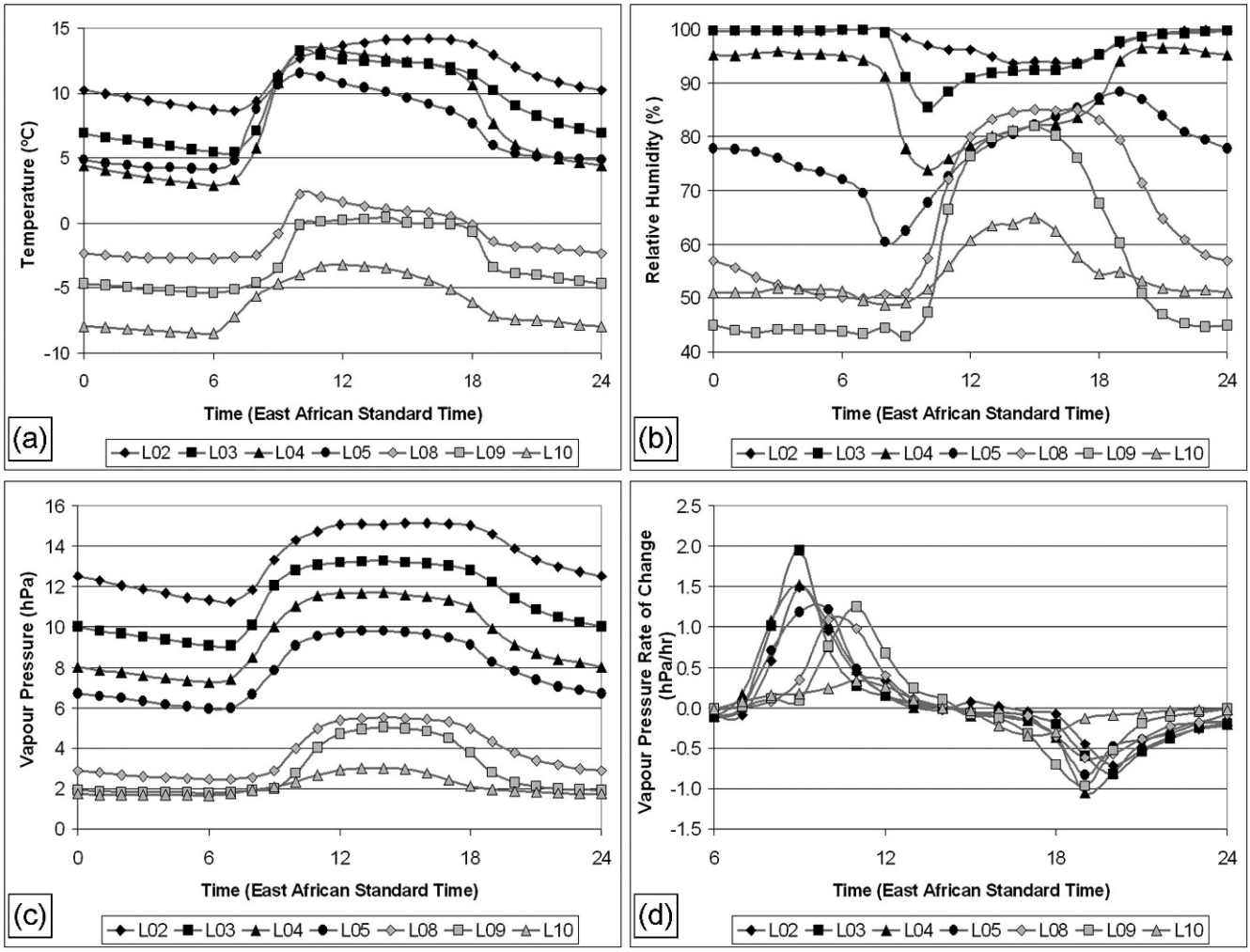


**FIGURE 9. Mean diurnal regimes of (a) air temperature, (b) relative humidity, (c) absolute vapor pressure, and (d) rate of change of vapor pressure.**

Further details of upslope moisture transport are represented in Figure 10. The relative humidity increases at higher altitudes throughout the morning and early afternoon. The largest changes between the hours of 08:00 and 14:00 take place around 5200 m. Site 10 shows a much subdued daily cycle, possibly due to the stabilizing influence of the ice surface providing a constant supply of moisture to the atmosphere (Mölg and Hardy, 2004).

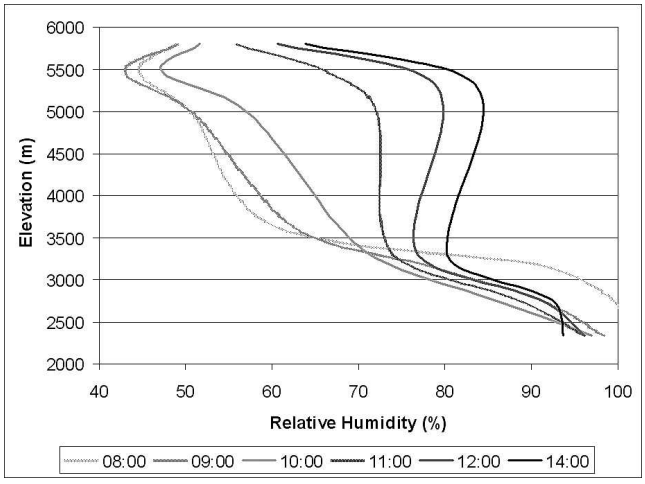


**FIGURE 10. Vertical profiles of relative humidity by time, showing increased levels at higher elevations through midday and into early afternoon.**

## *CLOUD REGIMES*

Following preliminary calibration between site 10 humidity data and over 100 automated camera images showing fog on the Northern Icefield (Hardy, unpublished), a threshold of 95% relative humidity has been used to define a high probability of cloud presence at individual logger locations, allowing subsequent analysis of cloud frequencies on Kilimanjaro with respect to altitude. This value is not prescriptive as our findings show that sensitivity to the exact threshold is low.

The cloud regime on Kilimanjaro shows strong diurnal forcing (Fig. 11). The *y*-axis represents the percentage frequency of days with cloud cover (RH $>$ 95%) at each hour (total number of days = 492). Lower slope sites are almost perpetually in cloud throughout the night, with brief clearance usually during daytime hours. As noted previously a persistent low level inversion results in a stratocumulus layer wreathing the forest zone, particularly during the period of southeast trade winds (June–August) when this side of the mountain is directly exposed to the prevailing flow. On over 80% of days, cloud dissipates at site 4 (in the vicinity of treeline) shortly after sunrise, while at site 3 this happens on only 40–50% of mornings. The decrease in cloud frequencies with altitude at this time of the day indicates evaporation of clouds

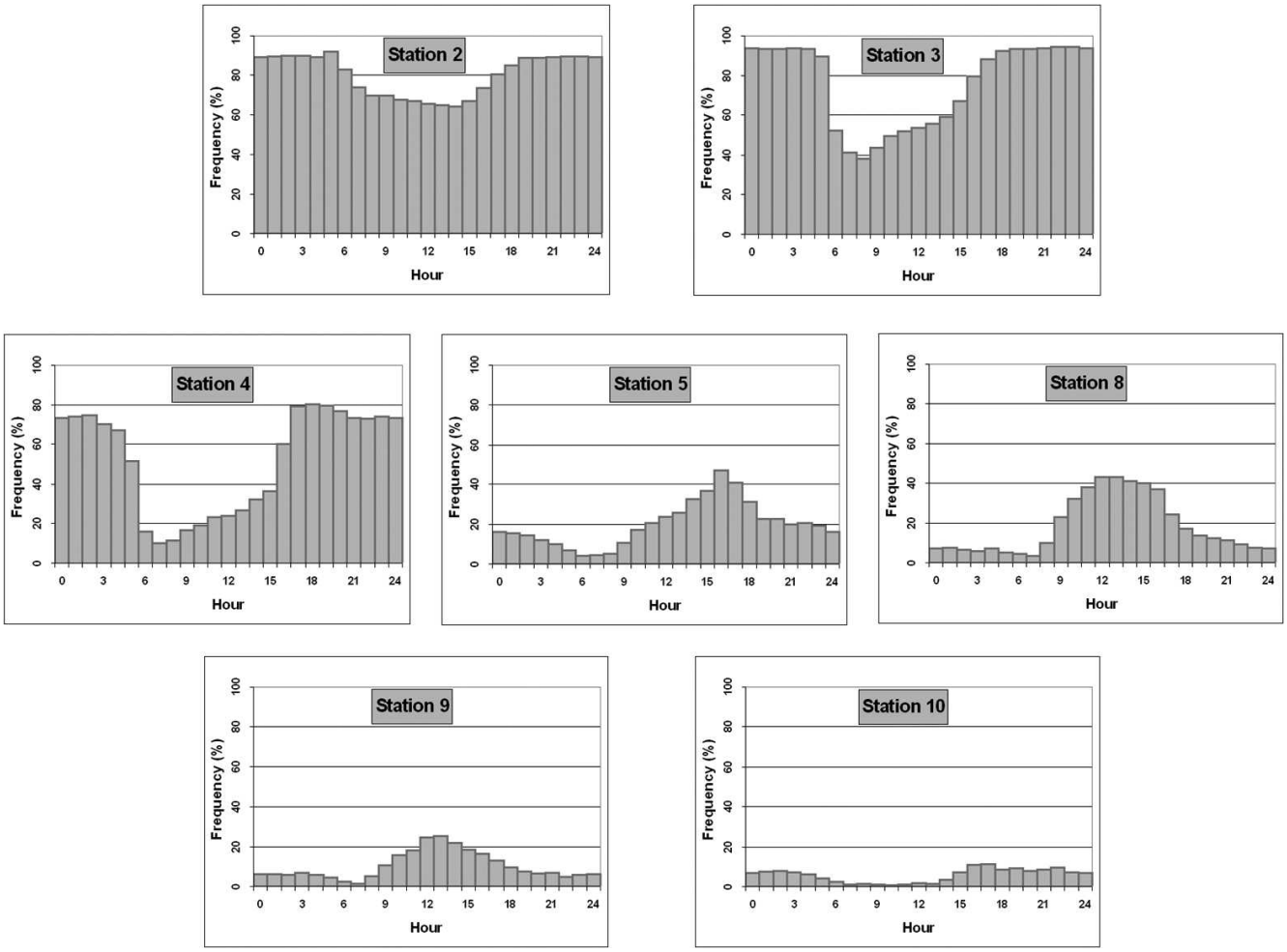


**FIGURE 11. The percentage of days with cloud cover (RH > 95%) at each location for all months.**

from above through solar heating. The higher sites show much lower cloud frequencies overall, but there is appearance of cloud during the afternoon on many days, presumably moving upslope under convection. Interestingly, the number of days on which this occurs decreases at the higher sites, suggesting that cloud development remains below the crater on many occasions.

In addition, site 10 on the Northern Icefield appears decoupled from the behavior at sites 8 and 9, with a much delayed and subdued daytime increase in cloud cover frequency, as hypothesized by Kaser and Osmaston (2002). There is a pronounced minimum in cloud frequency from 06:00 until 14:00 EAT (remaining below 5%) when the solar input would be intense. This would certainly enhance surface ablation of the ice field and the representativeness of this finding regarding lack of daytime cloud requires further research. If the lack of cloud is real (rather than a result of instrumental or calibration error), then there are many possible reasons why upslope clouds do not regularly appear at this location. These include local subsidence induced by topography in the crater; local surface cooling and suppression of convection induced by the ice field; persistent formation of the mean condensation level well below the crater; and/or strong advection of cool dry air blowing across the top of the crater preventing incursions of moist upslope air. The latter possibility was discussed by Garreaud et al. (2003) in their study on the Altiplano using a mesoscale model to evaluate effects of large scale flow aloft on moisture availability at high altitudes.

Mean annual figures disguise the variation between seasons. Similar graphs for January (northeast trade winds) and July (southeast trade winds) are shown for stations 2, 4, 8, and 10 in Figure 12. The two seasons are very different, with the persistent low level cloud cover failing to move upslope in July, particularly evident from observations at site 8, suggesting increased stability and lack of cloud development, but readily doing so in January when steeper lapse rates and strong surface heating occur. Clearly the two "dry" seasons have different upper level moisture and cloud regimes, which will have strong implications for conditions at the top of the mountain.

## Discussion and Implications

This paper has outlined the variation in temperature and relative humidity based on an altitudinal transect up the southwestern side of Kilimanjaro. It is clear that linear models of changes in atmospheric conditions based on elevation alone would be unsuitable due to decoupling of behavior at high and low elevations.

The importance of the forest/heathland transition in modifying the climate in the zone between sites 3, 4, and 5 cannot be overstated and would be of fundamental importance in understanding treeline dynamics and climate feedback mechanisms. Another marked non-linearity occurs in the transition from the rock scree to the ice field, conditions on the Northern Icefield (site 10) being very different from lower elevations. Thus extrapolation of summit climate from lower sites would be dangerous, confirming the need for detailed climate monitoring at a variety of elevations on such a mountain.

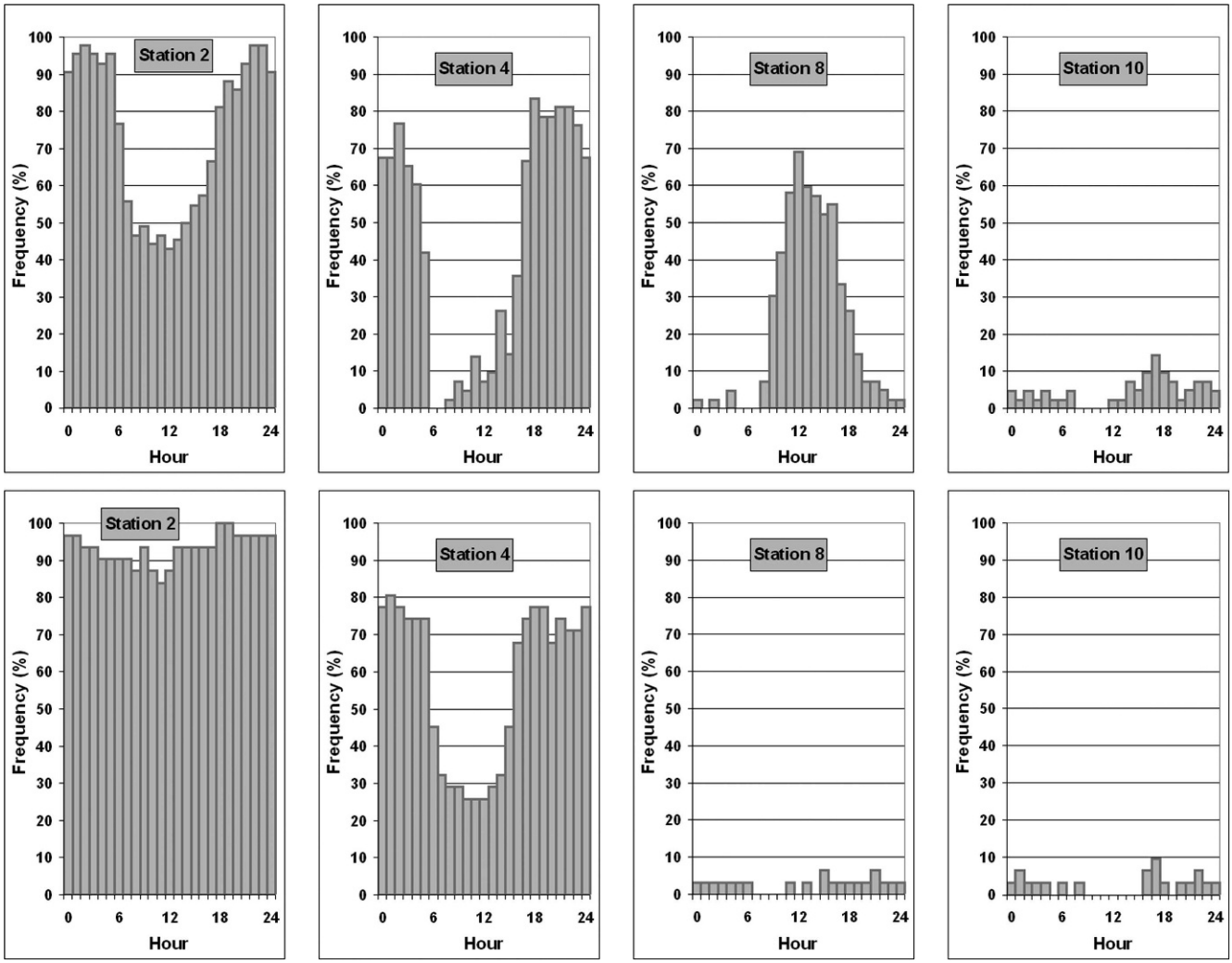


**FIGURE 12. As in Figure 10 but for January (top row) and July (bottom row) for selected stations. The total number of January days with data is 42 and for July is 31.**

It has been argued (Kaser et al., 2004; Mölg and Hardy, 2004; Cullen et al., 2006) that the reasons for the rapid decline in Kilimanjaro's glaciers are not primarily due to increased air temperatures, but a lack of precipitation. Indeed our data show that temperatures remain well below freezing at site 10, with daytime maxima averaging −2.1°C. Such low air temperatures keep sensible heat supply to the glacier small and make radiative exchanges more significant (Mölg and Hardy, 2004). Thus, patterns of cloud cover and humidity are central to understanding glacier-climate interactions (Mölg et al., 2003). Our data also suggest an absence of frequent daytime cloud cover at glacier level (Fig. 11), despite transport of moisture up the mountain and the frequent development of convective cloud at lower sites. Whether this has always been the case, or whether pronounced drying in recent decades has caused this we cannot prove, but we can offer some salient comments.

Nearly all of the moisture in the atmosphere at the higher levels of the mountain is brought up from lower elevations through the mechanism of the montane thermal circulation. Our data points strongly to the lower slopes of Kilimanjaro as a moisture source for both the snows that feed the summit glaciers and the clouds that impact their surface energy balance. The mean diurnal change in absolute vapor pressure is not that dissimilar in the forest zone to that at higher elevations, but by logic the forest is where daytime evapotranspiration should be at its peak (i.e. this is the major source zone for moisture). The lack of a damping of the diurnal amplitude in vapor pressure toward higher elevations (Fig. 7c) suggests net export of moisture out of the forest zone (upslope) during daylight hours. Over time it could be that land-use changes in the forest zone as a result of deforestation have reduced the efficiency of this moisture supply to the higher reaches of the mountain. There has been a substantial program of forest clearance in Tanzania since the 1970s and the mean rate of loss is reported as 412,000 ha $yr^{-1}$ over the last 5 years (2000–2005) (FAO, 2006). On Kilimanjaro there is also evidence to suggest a depression in the treeline due to increased bushfire frequency and intensity over the last 20–30 years (Hemp, 2005b), and drying as a result of deforestation and land-use change has been proposed in many other locations (Kanae et al., 2001; Pitman et al., 2004).

Further work is required to see the extent to which more detailed observations of cloud amount and type can be derived from our logger data. This is underway and involves more extensive calibration of our data with automated camera images, supplemental meteorological data taken by an automatic weather station on the Northern Icefield, as well as reanalysis and radiosonde data.

Our work has already shown the importance of moisture transport upslope to the summit of Kilimanjaro. The extent to which any long-term changes in moisture are locally controlled (rather than a result of changing free atmospheric conditions associated with variable advection) is a critical area for further research. This is being examined through a comparison of our

mountain surface data with free-air data from equivalent elevations. These are available from radiosonde sites at Nairobi Dagoretti 220 km to the north in Kenya and Dar Es Salaam 450 km to the southeast, and from reanalysis fields. The extent to which climate on the mountain becomes decoupled from the more regional atmospheric properties is an important focus. We would also like to know how representative our transect up the southwest side of the mountain is of conditions elsewhere, since the mountain atmosphere and resultant thermal circulation are suspected to be asymmetrical. We therefore hope to expand our sampling network to other slopes of the mountain. Surface data on the montane thermal circulation (particularly the development of anabatic and katabatic winds and their relationship to moisture advection) would also be of great use, even over a short period.

## Acknowledgments

This research is based in part on work supported by the National Science Foundation and NOAA Office of Global Programs, Climate Change Data and Detection Program (Grant no. 0402557, awarded to DRH). Equipment was generously supplied by the Department of Geography, University of Portsmouth and the Mountain Research Station, University of Colorado.

## References Cited

Bradley, R. S., Keimig, F. T., and Diaz, H. F., 2004: Projected temperature changes along the American cordillera and the planned GCOS network. *Geophysical Research Letters*, 31(16): L16210, doi: 10.1029/2004GL020229.

Bradley, R., Vuille, M., Diaz, H. F., and Vergara, W., 2006: Threats to water supplies in the tropical Andes. *Science*, 312: 1755–1756.

Cullen, N. J., Mölg, T., Kaser, G., Hussein, K., Steffen, K., and Hardy, D. R., 2006: Kilimanjaro glaciers: recent areal extent from satellite data and new interpretation of observed 20th century retreat rates. *Geophysical Research Letters*, 33: L16502, doi: 10.1029/2006GL027084.

Diaz, H. F., and Bradley, R. S., 1997: Temperature variations during the last century at high elevation sites. *Climatic Change*, 36: 253–279.

Dreiseitl, E., 1988: Slope and free air temperature in the Inn Valley. *Meteorology and Atmospheric Physics*, 39: 25–41.

Durre, I., Vose, R. S., and Wuertz, D. B., 2006: Overview of the Integrated Global Radiosonde Archive. *Journal of Climate*, 19(1): 53–68.

FAO, 2006: *Global Forest Resources Assessment 2005: progress towards sustainable forest management*. Rome, Italy: Viale delle Terme di Caracalla, Food and Agriculture Organisation Forestry Paper 147, 348 pp.

Findlater, J., 1977: Observational aspects of the low-level cross-equatorial jet stream of the western Indian Ocean. *Pure and Applied Geophysics*, 115: 1251–1262.

Garreaud, R., Vuille, M., and Clement, A. C., 2003: The climate of the Altiplano: observed current conditions and mechanisms of the past. *Palaeogeography, Palaeoclimatology, Palaeoecology*, 194: 1–18.

Griffiths, J. F., 1972: *Climates of Africa*. New York: Elsevier Science.

Hastenrath, S., 2001: Variations of East African climate during the past two centuries. *Climatic Change*, 50: 209–217.

Hemp, A., 2002: Ecology of the pteridophytes on the southern slopes of Mt. Kilimanjaro—I. Altitudinal distribution. *Plant Ecology*, 159(2): 211–39.

Hemp, A., 2005a: Continuum or zonation? Altitudinal gradients in the forest vegetation of Mt. Kilimanjaro. *Plant Ecology*. doi: 10.1007/s11258-005-9049-4.

Hemp, A., 2005b: Climate change–driven forest fires marginalize the impact of ice cap wasting on Kilimanjaro. *Global Change Biology*, 11: 1013–1023.

Hills, R. C., 1979: The structure of the Inter-Tropical Convergence Zone in equatorial Africa and its relationship to East African rainfall. *Transactions of the Institute of British Geographers*, 4(3): 329–352.

Kabanda, T. A., and Jury, M. R., 1999: Inter-annual variability of short rains over northern Tanzania. *Climate Research*, 13: 231–241.

Kanae, S., Oki, T., and Musake, K., 2001: Impact of deforestation on regional precipitation over the Indochina peninsula, *Journal of Hydrometeorology*, 2: 51–70.

Kaser, G., and Osmaston, H., 2002: *Tropical glaciers*. International Hydrology Series. Cambridge: Cambridge University Press, 207 pp.

Kaser, G., Hardy, D. R., Mölg, T., Bradley, R. S., and Hyera, T. M., 2004: Modern glacier retreat on Kilimanjaro as evidence of climate change: observations and facts. *International Journal of Climatology*, 24: 329–339.

Kuemmel, B., 1997. Temp, humidity and dew point ONA (http://www.faqs.org/faqs/meteorology/temp-dewpoint/). Accessed 7 May 2007.

Kuhnel, I., 1991: Cloudiness fluctuations over eastern Africa. *Meteorology and Atmospheric Physics*, 46: 185–195.

Latif, M., Dommenget, D., Dima, M., and Grötzner, A., 1999: The role of Indian Ocean SST in forcing East African rainfall anomalies during December/January 1997/98. *Journal of Climate*, 12: 3497–3504.

Mölg, T., and Hardy, D. R., 2004: Ablation and associated energy balance of a horizontal glacier surface on Kilimanjaro. *Journal of Geophysical Research*, 109: D16104, doi: 10.1029/2003JD004338.

Mölg, T., Hardy, D. R., and Kaser, G., 2003: Solar radiation maintained glacier recession on Kilimanjaro drawn from combined ice-radiation geometry modeling. *Journal of Geophysical Research*, 108: D23:4731, doi: 10.1029/2003JD003546.

Mölg, T., Renold, M., Vuille, M., Cullen, N. J., Stocker, T. F., and Kaser, G., 2006: Indian Ocean zonal mode activity in a multicentury integration of a coupled AOGCM consistent with climate proxy data. *Geophysical Research Letters*, 33: L18710, doi: 10.1029/2006GL026384.

NCDC, 2007: National Environmental Satellite Data Information Service (NESDIS) at the National Climate Data Center (http://www.ncdc.noaa.gov/oa/climate/igra/index.php). Accessed March 2007.

Pepin, N. C., and Losleben, M., 2002: Climate change in the Colorado Rocky Mountains: free air versus surface temperature trends. *International Journal of Climatology*, 22: 311–329.

Pepin, N. C., and Seidel, D. J., 2005: A global comparison of surface and free-air temperatures at high elevations. *Journal of Geophysical Research*, 110: D03104, doi: 10.1029/2004JD005047.

Pitman, A. J., Narisma, G. T., Pielke, S. A., Sr., and Holbrook, N. J., 2004: Impact of land cover change on the climate of southwest Western Australia, *Journal of Geophysical Research*, 109: D18109, doi: 10.1029/2003JD004347.

Plisnier, P. D., Serneels, S., and Lambin, E. F., 2000: Impact of ENSO on East African ecosystems: a multivariate analysis based on climate and remote sensing data. *Global Ecology and Biogeography*, 9(6): 481–497, doi: 10.1046/j.1365-2699.2000.00208.

Rohr, P. C., and Killingtveit, A., 2003: Rainfall distribution on the slopes of Mt. Kilimanjaro. *Journal of Hydrological Sciences*, 48(1): 65–77.

Ropelewski, C. F., and Halpert, M. S., 1987: Precipitation patterns associated with El Niño/Southern Oscillation. *Monthly Weather Review*, 115: 1606–1626.

Troll, C., and Wien, K., 1949: Der Lewisgletscher am Mount Kenya. *Geografiska Annaler*, 31: 257–274.

*Ms accepted August 2007*